

Electronic Supporting Information

A comprehensive study of electronic, optical, mechanical and piezoelectric properties of Li-based Tin-halide perovskites from GGA, Meta-GGA and HSE06

Celestine Lalengmawia^{1,2} Zosiamliana Renthlei^{1,2} Shivraj Gurung,² Lalhriat Zuala,² Lalrinthara Pachuau,² Ningthoujam Surajkumar Singh,² Lalmuanpuia Vanchhawng,² Karthik Gopi,³ A. Yvaz,⁴ and D. P. Rai²

1)Department of Physics, Mizoram University, Aizawl-796009, India

2)Physical Sciences Research Center (PSRC), Department of Physics, Pachhunga University College, Aizawl-796001, India

3)Department of Nuclear Physics, University of Madras, Guindy Campus, Chennai-600025, India

4)World-class research center “Advanced Digital Technologies”, State Marine Technical University, Saint Petersburg, 190121 Russia

*email: dibyaprakasrai@gmail.com.

Mulliken Population Analysis:

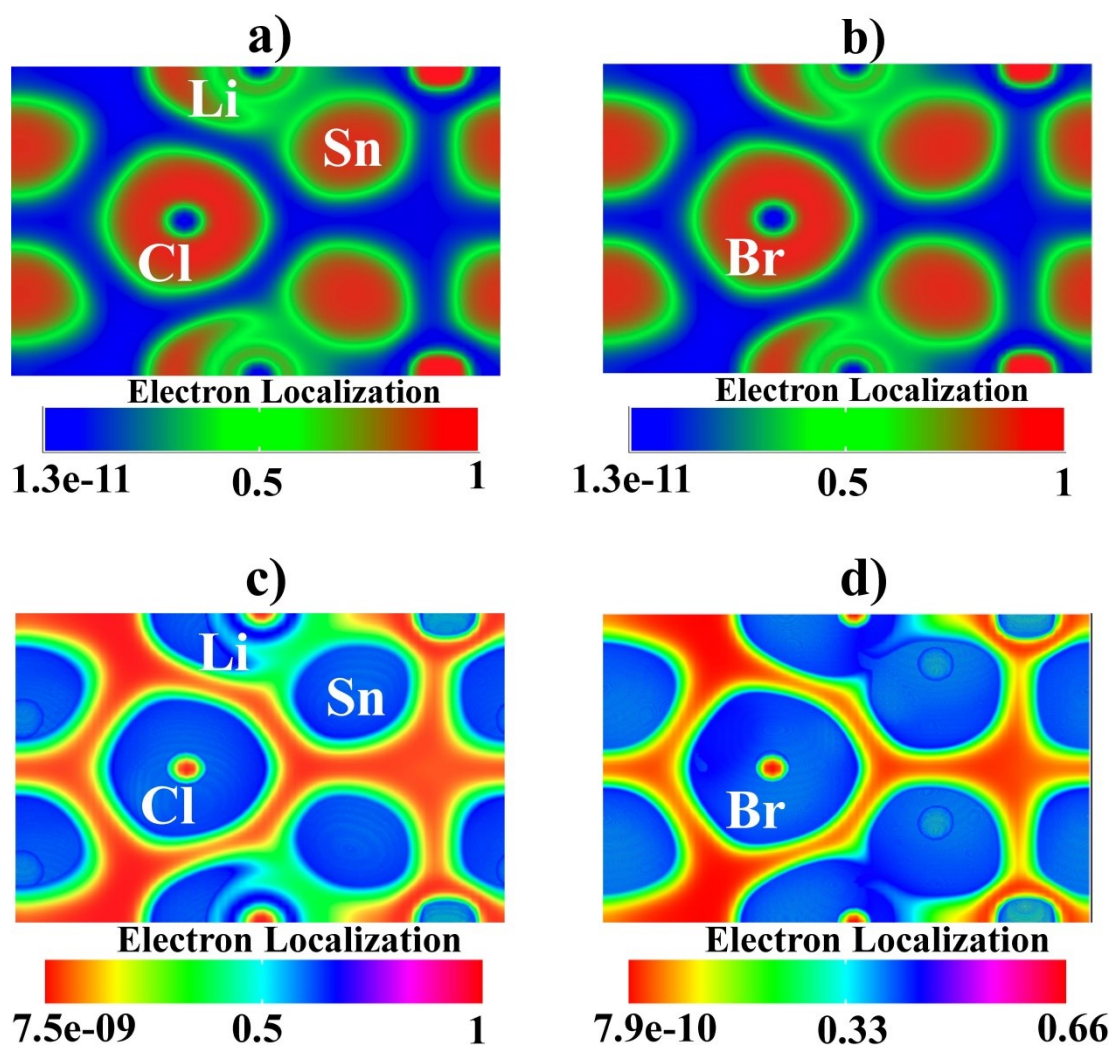
To understand the inter-atomic bonding within the compounds, we have utilized the mulliken population analysis (MPA) [1] which provides an insight of bonding between atoms and charge distributions among the atoms within the materials. Herein, Table S1 we report the analyzed populations, charges and bond lengths of the studied halide perovskites-LiSnCl₃ and LiSnBr₃ using GGA and mGGA. The contributions of all atoms are given in terms of their charges of s- and p-orbitals. The presence of negative charge values in Cl/Br atom is a result of charge accumulation which has a direct indication of charge transfer from Sn/Li→Br/Cl, creating charge depletion around Sn/Li atoms. The results of charge depletion (+) and charge accumulation (-) by using GGA and mGGA are given in Table S1

| Compound(s) | Functionals | Species | Atomic Population | | | Mulliken charge (e) | Bond | Bond length (Å) |
|---------------------|-------------|---------|-------------------|------|-------|---------------------|-------|-----------------|
| | | | Total | s | p | | | |
| LiSnCl ₃ | GGA | Li | 2.39 | 2.06 | 0.32 | (+)0.61 | Li-Sn | 3.41 |
| | | | | | | | Li-Cl | 2.67 |
| | | Sn | 13.35 | 0.15 | 11.41 | (+)0.65 | Sn-Cl | 2.63 |
| | | Cl | 7.41 | 1.93 | 5.48 | (-)0.41 | Cl-Cl | 3.46 |
| LiSnBr ₃ | GGA | Li | 2.51 | 2.15 | 0.37 | (+)0.49 | Li-Sn | 3.62 |
| | | | | | | | Li-Br | 2.85 |
| | | Sn | 13.49 | 1.95 | 11.54 | (+)0.51 | Sn-Br | 2.77 |
| | | Br | 7.33 | 1.94 | 5.39 | (-)0.33 | Br-Br | 3.72 |
| LiSnCl ₃ | mGGA | Li | 2.53 | 2.15 | 0.38 | (+)0.47 | Li-Sn | 3.98 |
| | | | | | | | Li-Cl | 2.44 |
| | | Sn | 13.38 | 1.90 | 11.48 | (+)0.62 | Sn-Cl | 2.58 |
| | | Cl | 7.37 | 1.90 | 5.49 | (-)0.37 | Cl-Cl | 3.39 |
| LiSnBr ₃ | mGGA | Li | 2.56 | 2.21 | 0.35 | (+)0.44 | Li-Sn | 3.59 |
| | | | | | | | Li-Br | 2.69 |
| | | Sn | 13.46 | 1.92 | 11.55 | (+)0.54 | Sn-Br | 2.73 |
| | | Br | 7.32 | 1.93 | 5.39 | (+)0.32 | Br-Br | 3.70 |

Table S1: Calculated the atomic populations, mulliken charge and bond lengths of LiSnX₃ (X = Cl, and Br) using GGA and mGGA

Electron Localization Function

The electron localization function (ELF) [2] has become an effective tool for qualitatively comprehending the behaviour of electrons within the atomic system during the course of crystalline formation. A wide range of bonding scenarios can be explained, from the most common covalent to the metallic bond. The ELF does not solely depend on the employed basis sets and computational techniques. ELF plays a crucial role in understanding the chemical bond formation providing vital information about the electrons localization. We have displayed the 2D and 3D ELF maps of LiSnCl_3 and LiSnBr_3 employing GGA and mGGA in Fig.S1. As seen from the figures obtained using GGA, the region with the red colour reveals higher electron localization while the blue colour displays the regions with lower electron localization [see Fig. S1 (a-b) & Fig. S1 (e-f)]. Whereas, the representation of colour coding is just the opposite for mGGA as compared to GGA [see Fig.S1 (c-d) & Fig. S1(g-h)]. The charge localizations are more in Cl- and Br-atoms due to their higher level of electronegativity than Li and Sn atoms. Thus, these findings support the results of the Mulliken population analysis.



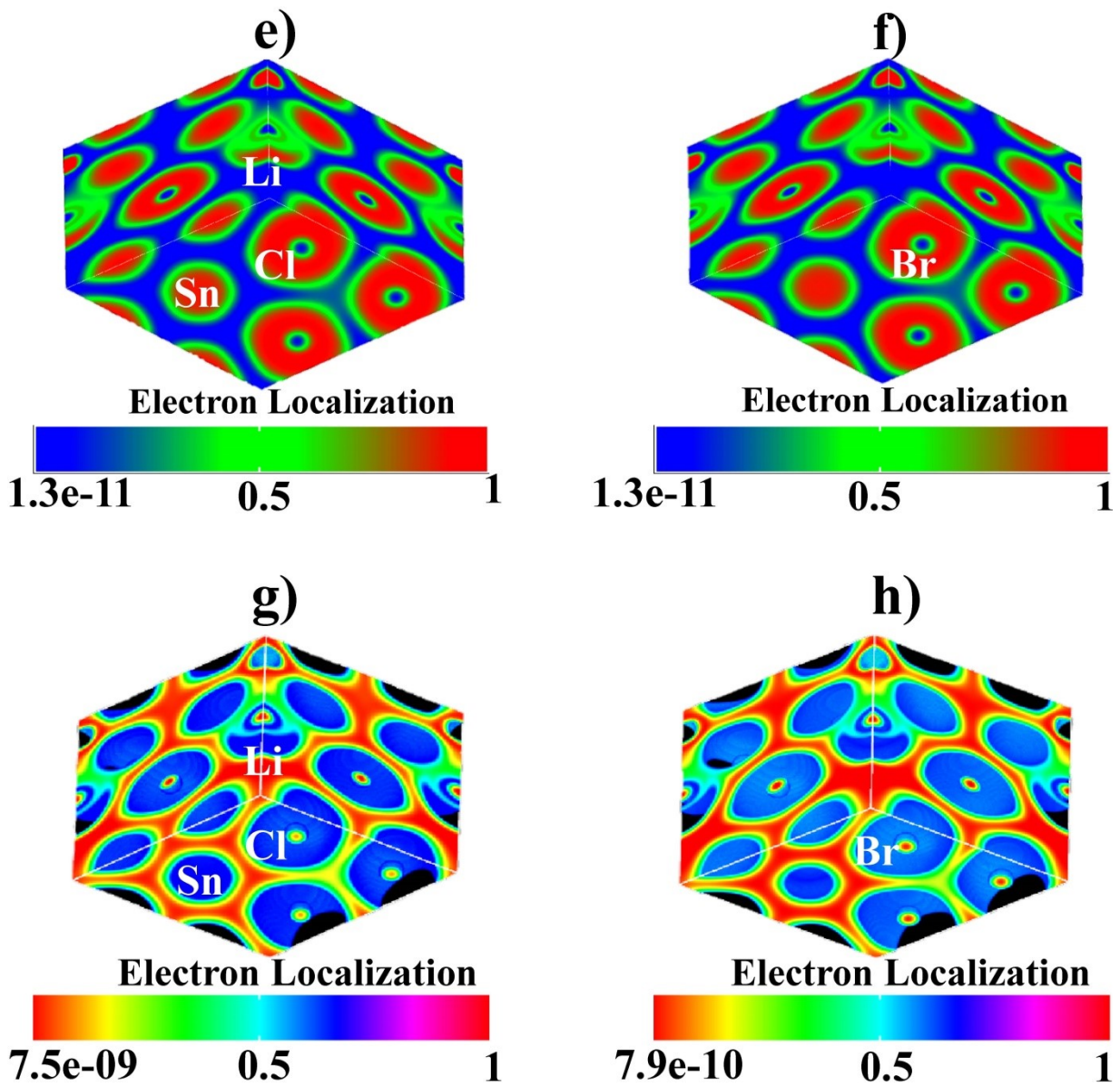
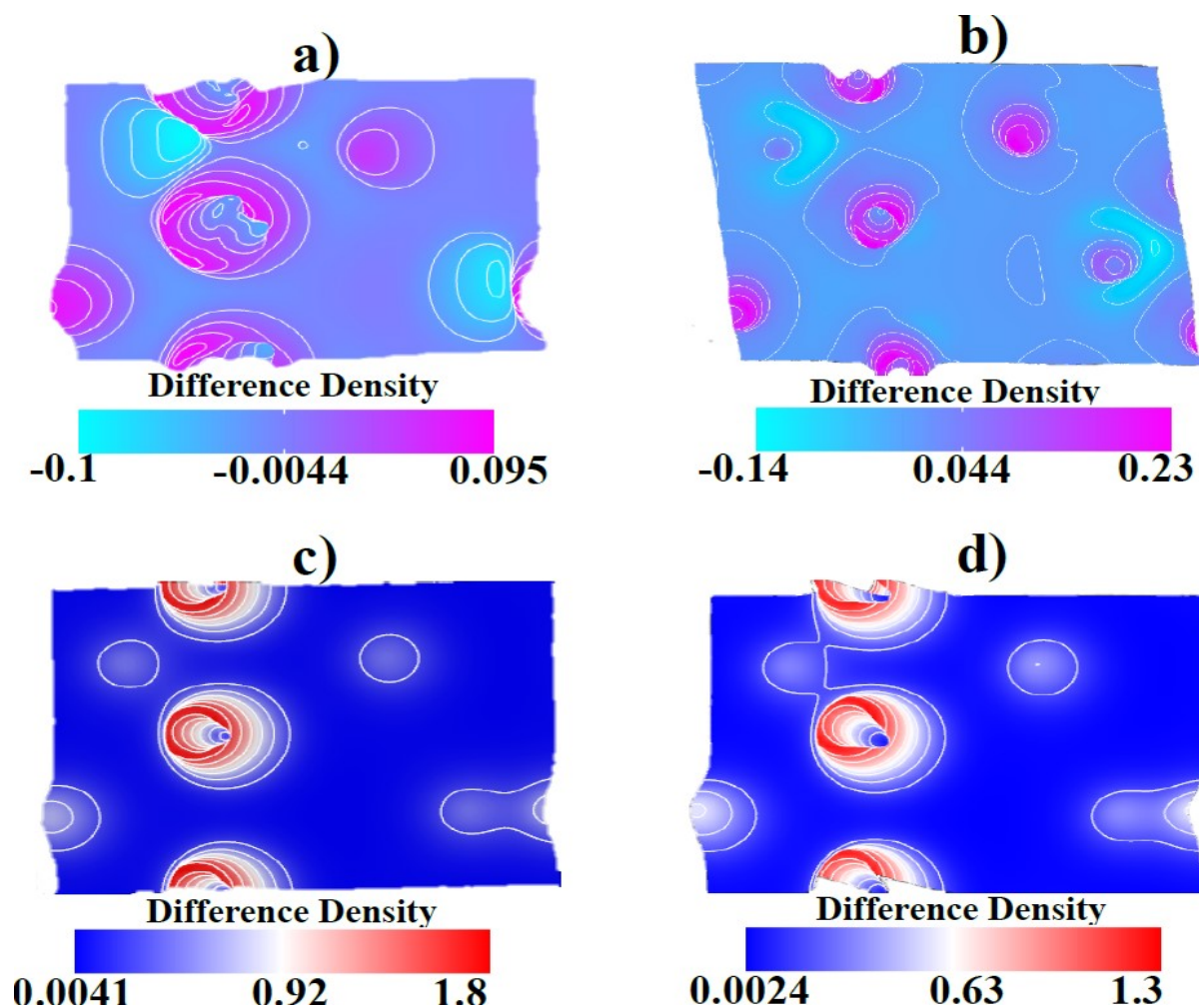


Fig.S1: 2D & 3D schematic presentation of Electron Localization Function (ELF) for LiSnX_3 where Fig.(a-b & e-f) are obtained using GGA and Fig.(c-d & g-h) are obtained using mGGA

Electron Difference Density (EDD):

Electron Difference Density (EDD)[3] also plays a vital role in chemical bonding as it compares the electron densities between the atoms within the materials. EDD provides valuable information about the electronic structures with the allocations of the charge between Li, Sn, Cl, and Br atoms. Within the system, the recombination of atoms will produce charge transfer which produces fascinating outcomes. The obtained figures in 2D and 3D, using GGA FigS2.(a-b, e-f) & Fig.(c-d, g-h) using mGGA, depicts the distribution of charge within the materials. From our output figures obtained using GGA, we have observed that the regions with magenta color reveals higher densities of electrons while regions having light blue color depicts lower in densities of the electrons. But in the 3D contour plot Fig.S2.(g), we observed that there are atleast two lower points which shows less accumulation of charge as compared to the other regions. These particular areas are considered to be having the weakest bond while the crystalline formation. Likewise, from the figures obtained employing mGGA, we also noted the regions tends to red color are considered to have accumulated more electrons then the ones tending towards the blue color. Therefore, we have come to know that the findings of MPA, ELF and EDD are in good agreements with another.



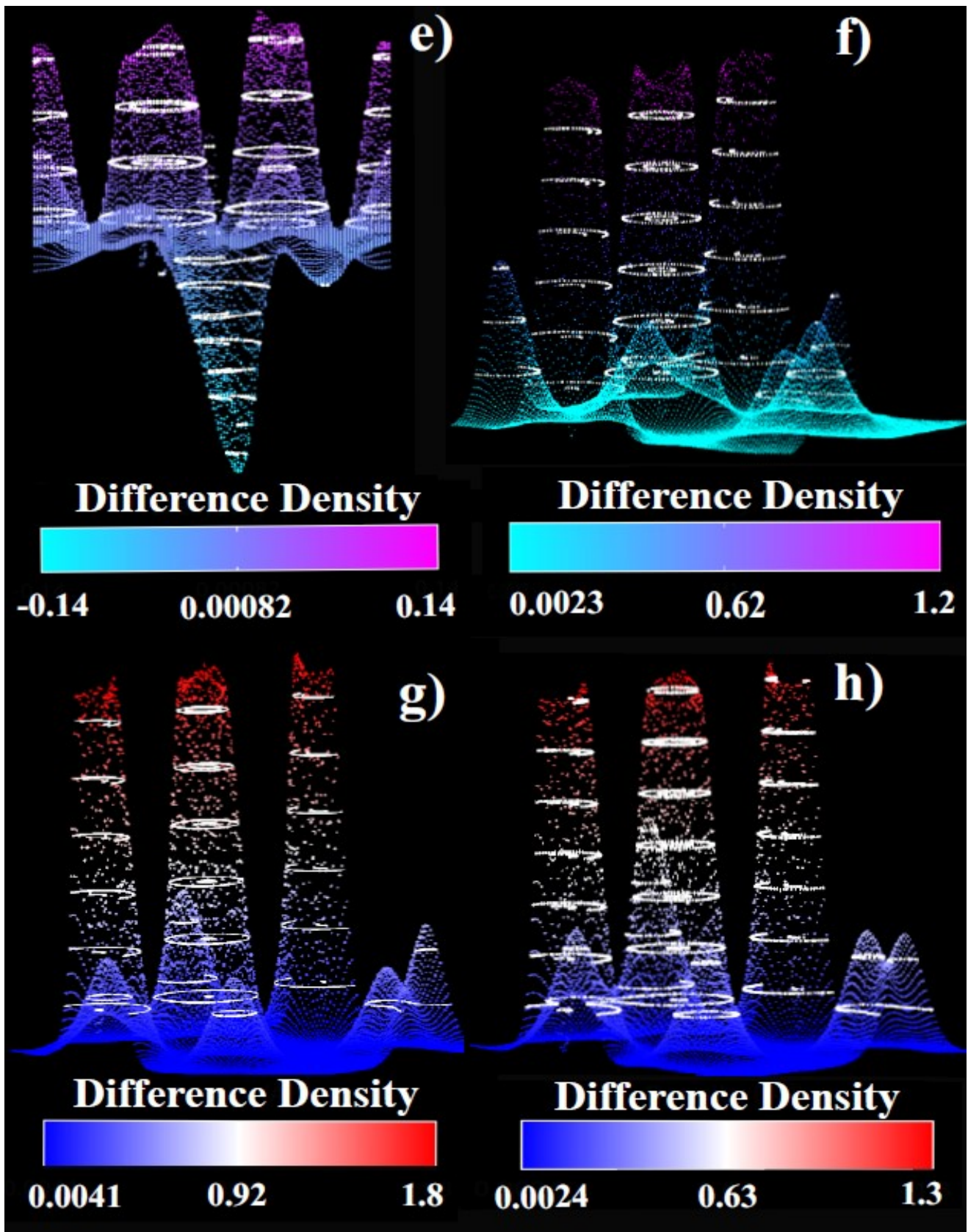


Fig.S2: 2D & 3D schematic presentation of Electron Difference Density (EDD) for LiSnX_3 where Fig.(a-b & e-f) are obtained using GGA and Fig.(c-d & g-h) are obtained using mGGA

Optical Properties: Dielectric constants, Absorption Coefficients, and Optical Conductivities (all along zz-direction) and Refractive Indices of LiSnX_3 (X = Cl and Br)

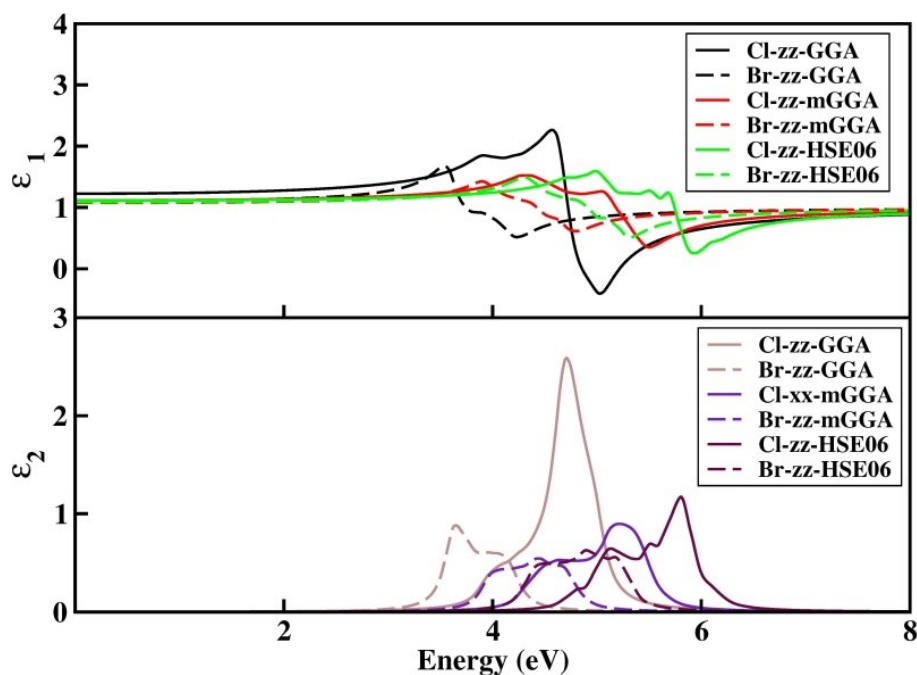


Fig.S3: Calculated Dielectric Constants of LiSnX_3 (X= Cl and Br) using GGA, mGGA and HSE06

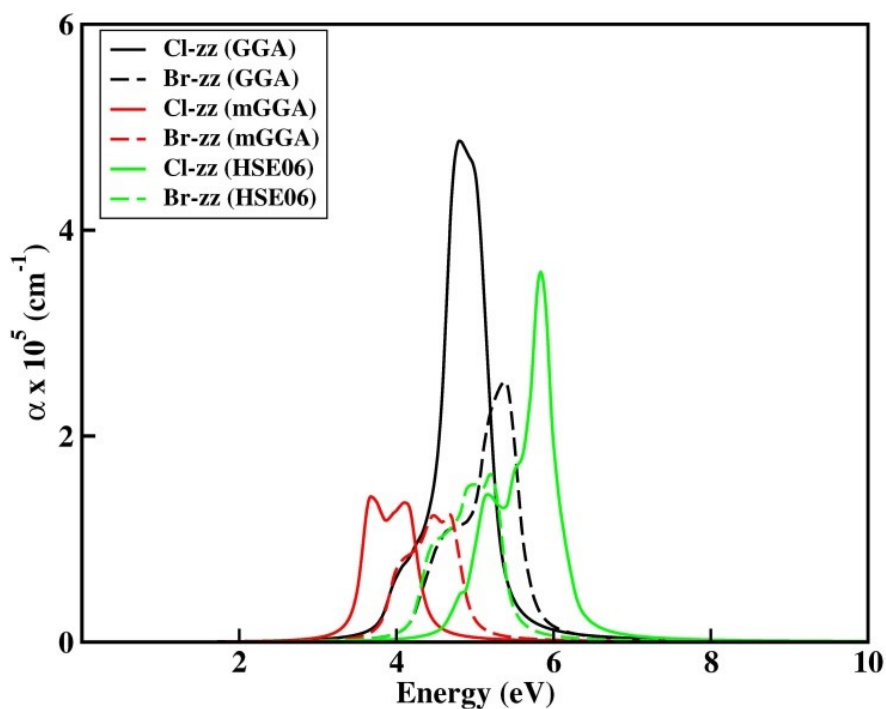


Fig.S4: Calculated Absorption coefficients of LiSnX_3 (X= Cl and Br) using GGA, mGGA and HSE06

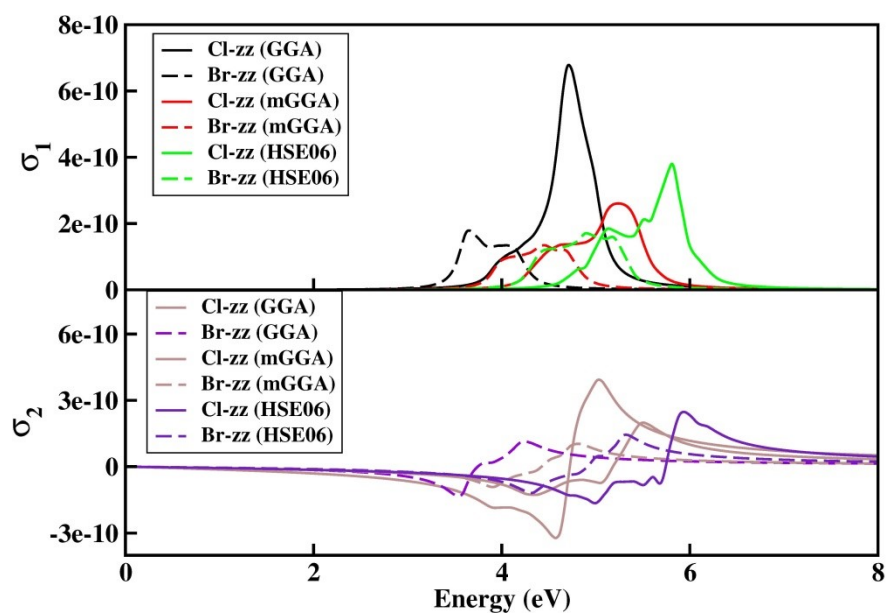


Fig.S5: Calculated Optical Conductivities of LiSnX_3 (X= Cl and Br) using GGA, mGGA and HSE06

Refractive Indices

The refractive index (η) [4] describes how light travels from one material to another. It illustrates how light's velocity drops when the refractive index of a material increases. This could be due to the interplay of atoms in the substrate and their effect on light. Herein, we obtained all the refractive indices of LiSnCl_3 and LiSnBr_3 using GGA, mGGA, and HSE06 functionals which are depicted in Fig.S6. The obtained figures are plotted in both xx- and zz- directions. From the figures, under the employed functional GGA, we observed that for $X = \text{Cl}$ along the xx- and zz-axes, the spectral peak reaches upto 1.52 a.u and 1.64 a.u at 3.86 eV and 4.75 eV, respectively. And for $X = \text{Br}$ (GGA), both the spectral peaks reaches upto 1.82 a.u at 3.85 eV and 1.31 a.u at 3.56 eV along xx- and zz- axes. Under employed mGGA, we also observed the peak upto 1.73 a.u and 1.17 a.u at 4.23 eV and 4.12 eV along xx- and zz-axes, respectively, for $X = \text{Cl}$. And for $X = \text{Br}$, the xx- and zz- direction reaches the level upto 1.38 a.u and 1.33 a.u at 3.89 eV and 3.68 eV. Similarly, for HSE06, we observed that the spectral peaks reaches upto 1.64 a.u and 1.23 a.u at 4.92 eV and 5.12 eV, respectively, along xx-and zz-axes ,for $X = \text{Cl}$. For $X = \text{Br}$, the peaks extends upto 1.52 a.u and 1.21 a.u at 4.23 eV and 4.12 eV along the xx- and zz- directions. The obtained index spectra closely resemble with the real parts (ϵ_1) of the dielectric constant, with the high peaks falling inside the vis-UV region.

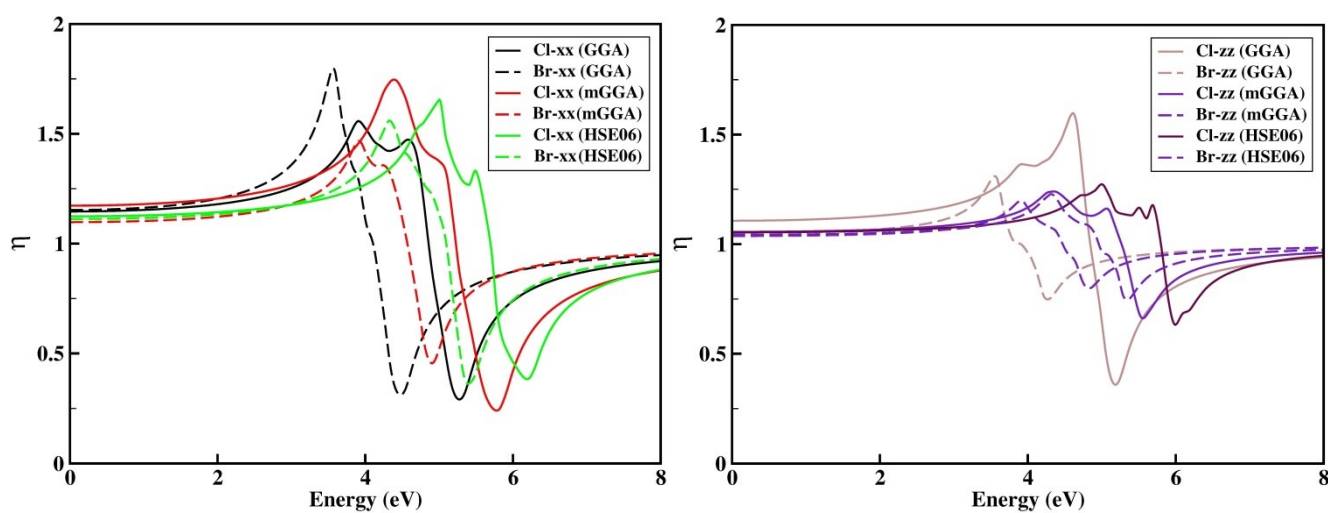


Fig.S6: Calculated refractive index of LiSnX_3 ($X = \text{Cl}$ and Br) along xx- and zz-axes using GGA, mGGA, and HSE06

Melting Temperature

Understanding a material's melting point is essential for real world applications. In addition to simulating atomic and ionic radii, the temperature parameter is crucial for structural stability. Using the following equation, we have obtained the melting temperatures (T_m) of the compounds studied[5].

$$T_m = 553 + 5.911C_{11} \pm 300 \quad (i)$$

As shown in Table S2, the calculated T_m values using GGA and mGGA are aligned, where LiSnCl_3 in both functionals have higher melting temperatures than LiSnBr_3 . Among them $X = \text{Cl}$ (mGGA) has the highest value up to 723.06 ± 300 K which simply means that it can out-stand its structural integrity even at high temperatures comparing with the others' values.

Sound Velocity

Determining sound velocities is one of the important parameters in estimating mechanical properties[6]. They can be obtained by using the crystal symmetry and the direction of propagation. The longitudinal velocities, $v_l = [(B + 4G/3)/\rho]^{1/2}$ and transverse velocities, $v_t = (G/\rho)^{1/2}$, also known as the seismic-compression and shear waves are used to obtain the mean sound velocities v_m

$$v_m = [(1/v^3_p + 2/v^3_s)/3]^{-1/3} \quad (ii)$$

Our calculated results for v_l , v_t and v_m are presented in Table S2. We observed that among the compounds studied, $X = \text{Cl}$ (GGA) has the highest v_l value while $X = \text{Cl}$ (mGGA) has the highest v_t value. The highest mean sound velocities are obtained by $X = \text{Cl}$ (mGGA) with the value of 1450 m/s. The true forms of hexagonal crystals can only be obtained in [100] and [001] directions. These can be derived using the following equations

$$\begin{aligned} [100] : [100]v_l &= \sqrt{(C_{11} - C_{12})/2\rho} \\ [010]v_{t1} &= \sqrt{C_{11}/\rho} \end{aligned} \quad (iii)$$

$$[001]v_{t2} = \sqrt{C_{44}/\rho}$$

$$\begin{aligned} [001] : [001]v_l &= \sqrt{C_{33}/\rho} \\ [100]v_{t1} &= \sqrt{C_{44}/\rho} \end{aligned} \quad (iv)$$

$$[010]v_{t2} = \sqrt{C_{44}/\rho}$$

Utilizing the above two equations (iii) and (iv), we obtained the sound velocities values for these compounds in the directions of x[100] and z[001], respectively. In the equations, the first and second transverse modes are represented by v_{t1} and v_{t2} , respectively. As listed in Table S3, along the [100] propagation direction, X= Cl (GGA) has the highest sound velocity at [010] v_{t1} polarization direction while the smallest value results along [001] v_{t2} polarization direction of X = Br (GGA). Along the propagation direction [001], again X = Cl (GGA) tops the sound velocity and the polarization directions along [100] v_{t1} and [010] v_{t2} possess identical sound velocities. Thus, in the study of sound velocities, GGA has a greater impact on these compounds studied.

| X | Functional | V_l | V_t | V_m | T_m | V_D | θ_D |
|----|------------|-------|-------|-------|--------|-------|------------|
| Cl | GGA | 2960 | 1250 | 1410 | 717.08 | 3.4 | 163.1 |
| Br | GGA | 1500 | 1030 | 1120 | 684.93 | 2.8 | 134.3 |
| Cl | mGGA | 2400 | 1290 | 1450 | 723.06 | 3.5 | 167.9 |
| Br | mGGA | 1620 | 940 | 1040 | 631.67 | 2.5 | 119.9 |

Table S2: Calculated values of longitudinal wave (V_l), transverse wave (V_t) and mean sound velocities (V_m). All waves and sound velocities are in m/s. Melting temperature (T_m , ± 300) (in K), machinability index (μ), Debye's frequency(V_D)($\times 10^{12}$) in Hz and Debye's Temperature(θ_D) in K.

Debye's Temperature and Frequency

In material science, Debye temperature (θ_D) is a crucial metric that helps to understand how materials behave under extreme heat and cold. It also sheds light on the mechanical and thermal characteristics of materials. The θ_D also indicates the toughness of a material and can even dictate the number of active phonon modes through its relationship with sound velocities, density and

mass of the material. This phenomenon can be activated by the crystal's structure, chemical composition, and other external factors such as pressure and temperature. Using the following equation, we can obtain the Debye's temperature of the materials.

$$\theta_D = \frac{h\nu_D}{k} \quad (v)$$

where h is the Planck's constant, ν_D is Debye's frequency, and k denotes the Boltzmann constant.

In order to acquire to the value of θ_D , first we need to have the debye's frequency ν_D , which depends solely on the number of atoms per unit volume and the sound velocities. The equation given below can be utilized to obtain the debye frequency.

$$\nu_D^3 = 2\pi \cdot 9 (N/V) \left[\frac{2}{v_t^3} + \frac{1}{v_l^3} \right]^{-1} \quad (vi)$$

Using Equations (v) and (vi), we calculated the values of Debye's temperatures and frequencies of the lead-free halide compounds presented in Table S2. We observed that X = Cl (mGGA) has the highest values of ν_D and θ_D which signifies that it has the best mechanical attributes and can stand up to temperate conditions compared to the others[7].

| X | Functionals | [100] | | | [001] | | |
|----------|--------------------|--------------|---------------|---------------|--------------|---------------|---------------|
| | | $[100]v_l$ | $[010]v_{l1}$ | $[001]v_{l2}$ | $[001]v_l$ | $[100]v_{t1}$ | $[010]v_{t2}$ |
| Cl | GGA | 1.73 | 3.06 | 0.84 | 2.76 | 0.84 | 0.84 |
| Br | GGA | 1.12 | 1.92 | 0.45 | 1.71 | 0.45 | 0.45 |
| Cl | mGGA | 1.37 | 2.73 | 1.25 | 2.59 | 1.25 | 1.25 |
| Br | mGGA | 0.61 | 1.48 | 0.58 | 1.67 | 0.58 | 0.58 |

Table S3: Calculated values of sound velocities for LiSnX_3 ($X = \text{Cl}$, and Br) along different directions [100] and [001].

1. Mulliken, R.S., *Electronic Population Analysis on LCAO–MO Molecular Wave Functions. I.* The Journal of Chemical Physics, 1955. **23**(10): p. 1833-1840.
2. Savin, A., et al., *ELF: The Electron Localization Function.* Angewandte Chemie International Edition in English, 1997. **36**(17): p. 1808-1832.
3. Steiner, E., *Density-difference maps in quantum chemistry.* Theoretica chimica acta, 1982. **60**(6): p. 561-572.
4. Wang, Q., et al., *Validation of Density Functional Theory Methods for Predicting the Optical Properties of Cu-Based Multinary Chalcogenide Semiconductors.* The Journal of Physical Chemistry C, 2022. **126**(9): p. 4684-4697.
5. Jung, J.H., et al., *High-accuracy thermodynamic properties to the melting point from ab initio calculations aided by machine-learning potentials.* npj Computational Materials, 2023. **9**(1): p. 3.
6. Celestine, L., et al., *A Halide-Based Perovskite CsGeX_3 ($X = \text{Cl}$, Br , and I) for Optoelectronic and Piezoelectric Applications.* Advanced Theory and Simulations, 2024. **7**(1): p. 2300566.
7. Chen, Q. and B. Sundman, *Calculation of debye temperature for crystalline structures—a case study on Ti, Zr, and Hf.* Acta Materialia, 2001. **49**(6): p. 947-961.